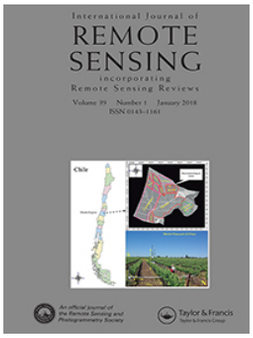

International Journal of Remote Sensing

ISSN: 0143-1161 (Print) 1366-5901 (Online) Journal homepage: https://www.tandfonline.com/loi/tres20

Estimation of gross primary production in Moso bamboo forest based on light-use efficiency derived from MODIS reflectance data

Yongjun Shi, Xiaojun Xu, Huaqiang Du, Guomo Zhou, Yufeng Zhou, Fangjie Mao, Xuejian Li & Dien Zhu

To cite this article: Yongjun Shi, Xiaojun Xu, Huaqiang Du, Guomo Zhou, Yufeng Zhou, Fangjie Mao, Xuejian Li & Dien Zhu (2018) Estimation of gross primary production in Moso bamboo forest based on light-use efficiency derived from MODIS reflectance data, International Journal of Remote Sensing, 39:1, 210-231, DOI: 10.1080/01431161.2017.1382747

To link to this article: https://doi.org/10.1080/01431161.2017.1382747

Published online: 25 Sep 2017.

INTERNATIONAL JOURNAL OF REMOTE SENSING, 2018
VOL. 39, NO. 1, 210–231
https://doi.org/10.1080/01431161.2017.1382747

Taylor & Francis
Taylor & Francis Group

Estimation of gross primary production in Moso bamboo forest based on light-use efficiency derived from MODIS reflectance data

Yongjun Shi[a,b,c], Xiaojun Xu[a,b,c], Huaqiang Du[a,b,c], Guomo Zhou[a,b,c], Yufeng Zhou[a,b,c], Fangjie Mao[a,b,c], Xuejian Li[b,c] and Dien Zhu[b,c]

[a]State Key Laboratory of Subtropical Silviculture, Zhejiang A & F University, Lin'an, China; [b]Key Laboratory of Carbon Cycling in Forest Ecosystems and Carbon Sequestration of Zhejiang Province, Zhejiang A & F University, Lin'an, China; [c]School of Environmental and Resources Science, Zhejiang A & F University, Lin'an, China

ABSTRACT

Assessing the contribution of Moso bamboo (*Phyllostachys pubescens*) forest to forest ecosystem carbon storage requires accurate estimation of gross primary production (GPP). Based on measurements of light-use efficiency (LUE), defined as the ratio of measured GPP to photosynthetically active radiation (PAR), from the eddy covariance flux tower, the linear regression model and partial least squares regression model were used for estimation of LUE using the Moderate-Resolution Imaging Spectroradiometer (MODIS) reflectance data. GPP estimates were then calculated by the product of LUE estimates and PAR (named the LUE-PAR model), which was compared with GPP from the GPP algorithm designed for the MODIS sensor aboard the Aqua and Terra platforms (MOD17A2 model) and the EC-LUE model. The results revealed the PLS model performed better than the linear regression model in LUE estimation but had lager uncertainties in high and low LUE values. GPP estimates driven by a MODIS-based radiation product with high spatial resolution was more accurate than those driven by Modern-Era Retrospective Analysis for Research and Applications (MERRA) radiation product from the NASA's Global Modelling and Assimilation Office data set. The LUE-PAR model had the highest accuracy than the other two LUE models. The GPP values derived from the EC-LUE model driven by photosynthetically active radiation (PAR) from MERRA and maximum LUE from the EC data were overestimated due to the overestimation in MERRA radiation product. The GPP values derived from the MOD17A2 model driven by PAR from the MERRA and maximum LUE from the biome properties look-up table were underestimated due to underestimation in the maximum LUE of Moso bamboo forest. This study implied that the LUE-PAR model driven by LUE estimates from the PLS model and PAR from MERRA is a superior approach in improving GPP simulations, and PAR products with high spatial resolution and accurate species-specific maximum LUE are necessary for the LUE models in estimating GPP at regional scale.

ARTICLE HISTORY
Received 31 March 2017
Accepted 11 September 2017

CONTACT Xiaojun Xu xuxiaojun3115371@163.com Zhejiang A&F University, 88# Huancheng North Road, Lin'an, Zhejiang Province 311300, China

1. Introduction

Gross primary production (GPP) of terrestrial ecosystems is a key part of terrestrial carbon cycle, which plays an important role in regulating the exchange of carbon between the atmosphere and terrestrial ecosystems and further global climate change (Zhao and Running 2010). Bamboo forest is one of important forest types in the world. The area of bamboo forest is about 37 million hectares in the world and accounts for roughly 1% of the global forest area in 2005 (Lobovikov et al. 2007). Moso bamboo (*Phyllostachys pubescens*) is a major bamboo species in China. A special characteristic of Moso bamboo forest is that production of new bamboo shoots fluctuated significantly among years (Li et al. 1998). According to the number of bamboo shoots, Moso bamboo forest can be classified as either on-year ('good' year) or off-year ('poor' year) bamboo forest, i.e. the year of bamboo shoot production is known as the on-year and the following year with less shoot production is known as the off-year (Li et al. 1998; Zhou et al. 2011). The number of bamboo shoots in an on-year is considerably greater than that in an off-year during mid-March to mid-May. On-year and off-year often alternated, forming a regular biennial cycle (Li et al. 1998). Leaf lifespan of Moso bamboo is two years, except in the first-year shoots where it is only one year (Li et al. 1998). Most of leaves in on-year are two years old leaves and those in off-year are one year old leaves. Two years old leaves and leaves on the first-year shoots are dropped in April (Li et al. 1998). Flushing of new leaves soon follows upon leaf dropping (Li et al. 1998). The characteristics of carbon storage of Moso bamboo forest are also different with other forest types. The height growth of bamboos is surprisingly rapid and arrives at their maximum height in about 40 days (Yen 2016). The biomass and soil carbon storage of Moso bamboo stands is strongly correlated with management strategies (Yen 2015; Li et al. 2013). Mean aboveground carbon sequestration value of Moso bamboo forests was higher than that of China fir plantations (Yen and Lee 2011). Many previous studies have demonstrated that Moso bamboo has a strong ability in absorbing carbon from the atmosphere and plays an important role in climate change mitigation (Chen et al. 2009; Komatsu et al. 2010; Lou et al. 2010; Li, Zhou et al. 2015). Accurate spatial and temporal GPP estimates of Moso bamboo are critical to understand and assess its contribution to forest carbon sequestration. Study on GPP estimation of Moso bamboo forest was rare and had considerable uncertainty in GPP estimates based on terrestrial carbon cycle model driven by remote sensing data (Xu et al. 2013).

Light-use efficiency (LUE) model is one kind of terrestrial carbon cycle models and has a firm ecophysiological basis, which is on the basis of strong relationship between GPP and the amount of solar energy the plants absorbed (Running and Zhao 2015). Many different LUE models were developed, such as the GPP algorithm designed for the MODIS sensor aboard the Aqua and Terra platforms (MOD17A2 model) (Running and Zhao 2015), Carnegie–Ames–Stanford approach (Potter et al. 1993), Vegetation Photosynthesis Model (Xiao et al. 2004), and Eddy Covariance-Light Use Efficiency (EC-LUE, Yuan et al. 2007). These LUE models have been widely used in estimating spatial distribution of GPP of forest ecosystem because they are simple and useful and easy to couple with remote-sensing data for large-scale application (Hilker et al. 2008; Yuan et al. 2014; Zhang et al. 2015). A key issue is to determine maximum LUE without environmental stress (ε_{max}), which is an important model parameter in the LUE models and significantly effects on the

accuracy of LUE models (Cheng et al. 2014). The ε_{max} varies widely with different vegetation types (Turner et al. 2003) and with different temporal-spatial pattern of same vegetation type (Hember et al. 2010). For regional studies, the ε_{max} should be carefully recalibrated and field-derived ε_{max} can be consistently applied to large-scale modelling (Xin et al. 2015). However, it is hard to get accurate and representative ε_{max} for regional studies through limited field inventory data and EC measurements, resulting in lager uncertainty in spatial variation of GPP estimates (Wang et al. 2010; Groenendijk et al. 2011; Keenan et al. 2012). Previous researches have shown that a direct estimation of LUE could reduce uncertainty of GPP estimates (Goerner, Reichstein, and Rambal 2009; Wu et al. 2012). Alternative approaches were presented to estimate proxy of LUE (such as chlorophyll content) or LUE using remote-sensing data (Gitelson et al. 2005, 2006; Wu et al. 2009; Peng et al. 2011), which has advantage in avoiding the issue of determining ε_{max} and can well represent the spatial heterogeneity of LUE. Estimation of chlorophyll content based on remote-sensing data has been proven feasible and can provide an acceptable accuracy because of the strong absorption by chlorophyll content in the visible blue and red regions (Gitelson et al. 2005; Peng et al. 2011). A good correlation has been found between canopy chlorophyll content and LUE for different vegetation types (Gitelson et al. 2006, 2014; Wu et al. 2009). Therefore, using remote-sensing data for LUE estimation is also feasible, which can provide spatial distribution of LUE and is a new possibility to estimate GPP (Wu et al. 2009, 2010, 2012).

In this study, the site-specific LUE of Moso bamboo forest was calculated based on GPP and photosynthetically available radiation (PAR) measurements from EC flux tower. Then, relationships between measured LUE and the Terra MODIS 8-day composite reflectance product (MOD09A1) were built using the empirical statistical models. GPP was estimated according to the product of predicted LUE and PAR and was then compared with GPP estimates derived from other LUE models. The objectives of this study are (1) to test the possibility for estimating LUE of Moso bamboo forest using MOD09A1 reflectance data, (2) to test the effect of PAR from different sources with different spatial resolution (observed PAR, PAR from the Modern-Era Retrospective Analysis for Research and Applications (MERRA) data set, and PAR estimates calculated from a solar radiation model) on accuracy of GPP estimates, and (3) to test the usefulness of the model in the estimation of GPP using MOD09A1 reflectance data and compare the model proposed in this study with different LUE models, such as the EC-LUE model and MOD17A2 algorithm.

2. Study area

The study area is located in Anji County, Zhejiang province, China, which is rich in Moso bamboo forest (Figure 1). Bamboo forest encompasses an area of 757 km^2 and accounts for 56.47% of the forested area, in which 79.30% is Moso bamboo. The canopy height of the Moso bamboo forest is approximately 11 m. The average annual precipitation is between 1100 and 1900 mm, and the average annual temperature is between 12.2°C and 15.6°C. An EC tower (30.476°N, 119.673°E) was built in 2010 to measure carbon fluxes of Moso bamboo forest because of large carbon sequestration potential for Moso bamboo forest. The 1000 × 1000 m square around the EC tower site comprises mainly Moso bamboo forest (86.1%) with small proportions of mixed forest (1.9%), cropland (8.6%), and buildings (3.4%). The site is surrounded by relatively complex terrain, ranging in

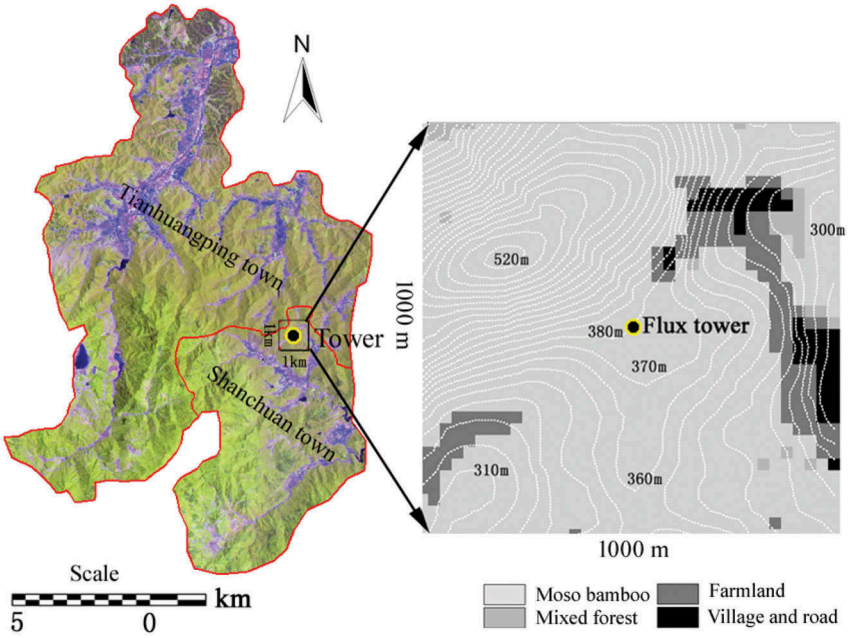

Figure 1. Study area and location of flux tower in Anji county, Zhejiang Province, China.

elevation from 288 to 525 m above sea level. The southern and southeastern region of the site is flat, whereas the northern and northwestern region is steeper. The EC system and its measurements are described in detail by Xu et al. (2013).

3. Materials and methods

In order to make this research design clear, a flow chart is shown in Figure 2. Table1 gives the explanations of those abbreviations shown in Figure 2.

3.1. *Acquisition of GPP and LUE*

The LUE of the canopy was defined as GPP divided by PAR in this study (Wu et al. 2009; Gamon, Serrano, and Surfus 1997). Daily GPP and PAR were calculated based on half-hourly values which were measured by the EC method and were corrected following the processing method introduced by Papale et al. (2006) using EdiRe and Matlab R2010b softwares. Missing half-hourly flux measurements were gap-filled based on the methods presented in Xu et al. (2013) and Lasslop et al. (2010). Daily values of GPP and PAR were indicated as missing if missing measurements accounted for greater than 20% of all data on a given day. The 8-day GPP and PAR were also calculated as the average value within 8-day period using daily GPP and PAR. The 8-day GPP and PAR were indicated as missing when missing daily GPP and LUE are greater than 40% of all data during the period of 8 days. Then, the 8-day LUE was calculated as 8-day GPP divided by 8-day PAR.

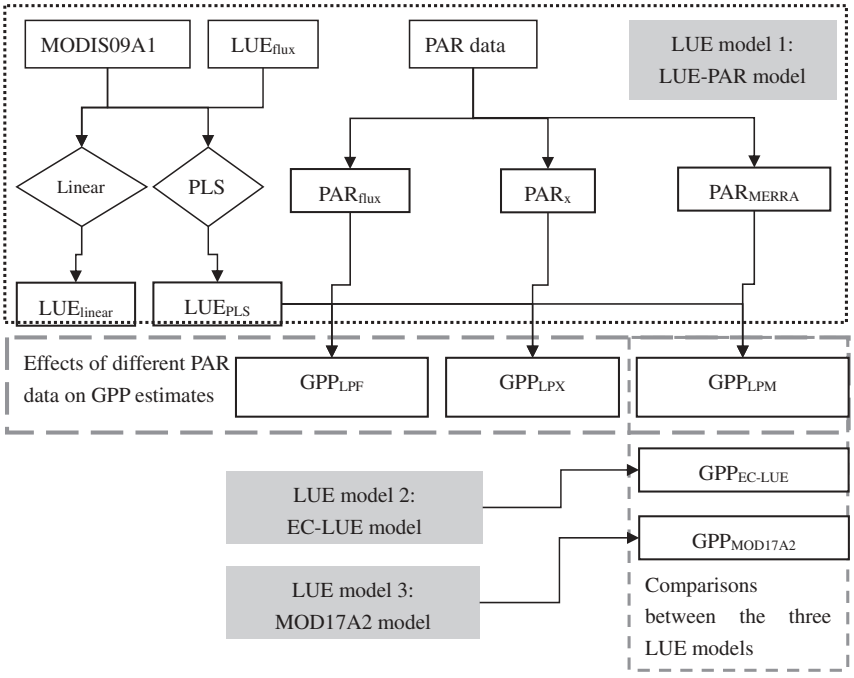

Figure 2. Flow chart of this research design.

Table 1. The explanations of those abbreviations shown in Figure 1.

Abbreviation	Full name	Explanation
LUE_{flux}	Observed LUE from the EC flux tower	Defined as GPP divided by PAR
LUE_{linear}	Estimated LUE using the linear regression	/
LUE_{PLS}	Estimated LUE using the partial least squares (PLS) regression	/
PAR_{flux}	Observed PAR from the EC flux tower	/
PAR_X	Estimated PAR from a solar radiation model	Spatial resolution of 1 km; Details in Xu, Du, Zhou, Mao et al. (2016)
PAR_{MERRA}	Estimated PAR from the MERRA dataset	Spatial resolution of 0.50° latitude by 0.67° longitude
GPP_{LPF}	Estimated GPP using the LUE-PAR model	Calculated as LUE_{PLS} multiplied by par_{flux}
GPP_{LPX}	Estimated GPP using the LUE-PAR model	Calculated as LUE_{PLS} multiplied by PAR_X
GPP_{LPM}	Estimated GPP using the LUE-PAR model	Calculated as LUE_{PLS} multiplied by PAR_{MERRA}
$GPP_{EC\text{-}LUE}$	Estimated GPP using the EC-LUE model	Driven by PAR_{MERRA}, maximum LUE calibrated by EC flux data
$GPP_{MOD17A2}$	Estimated GPP using the MOD17A2 model	Driven by PAR_{MERRA}, ε_{max} (1.05 g C m^{-2} day^{-1} MJ^{-1}) From the biome properties look-up table

3.2. *PAR data set*

Three kinds of surface incident shortwave radiation (SISR) data set were collected. The SISR is converted to PAR by multiplying by 0.45 for calculating GPP (Cai et al. 2014). The first one, named as PAR_{flux}, is measured using a CNR4 radiometer (4-Component Net

Radiometer, Kipp & Zonen, The Netherlands) located above the forest canopy layer at heights of 38 m above ground at EC flux tower site Anji. The second one, named as PAR_{MERRA}, is downloaded from the MERRA data set from http://gmao.gsfc.nasa.gov/research/merra/ with a spatial resolution of 0.50° latitude by 0.67° longitude. The third one, named as PAR_X, is average of the SISR from the MERRA data set and the SISR from a solar radiation model (Xu, Du, Zhou, Mao et al. 2016). The PAR_X has higher spatial resolution of 1 km and accuracy than PAR_{MERRA} (Xu, Du, Zhou, Mao et al. 2016).

3.3. *MODIS reflectance data and vegetation indices*

Surface reflectance data were acquired from the MOD09A1 at 500-m resolution and downloaded directly from the website of the Oak Ridge National Laboratory Distributed Active Archive Center. The MOD09A1 product includes seven bands: band 1 (red, 620–670 nm), band 2 (NIR, 841–876 nm), band 3 (blue, 459–479 nm), band 4 (green, 545–565 nm), band 5 (mid-IR, 1230–1250 nm), band 6 (mid-IR, 1628–1652 nm), and band 7 (mid-IR, 2105–2155 nm). There are uncertainties in MODIS reflectance data due to atmospheric effects, clouds, and snow. In order to remove bad reflectance data, blue band 3 reflectance data greater than 0.05, referred to the measured reflectance data of the forest canopy of Moso bamboo, were defined as bad data. Then, other band reflectance data were defined as bad if the blue band 3 reflectance data were bad. The raw MOD09A1 reflectance data and the values after the removal of the bad data are shown in Figure 3, which shows that the outliers were removed appropriately.

Based on MOD09A1 reflectance data, three important vegetation indices were calculated for estimating the LUE. Normalized difference vegetation index (NDVI, Equation (1)), enhanced vegetation index (EVI, Equation (2)), and simple ratio (SR, Equation (3)) are shown good relationships with LUE (Gitelson et al. 2006; Goerner, Reichstein, and Rambal 2009; Wu et al. 2009, 2012). Total 10 variables, including seven reflectance bands and three vegetation indices, were used to build models for estimating LUE. The three vegetation indices can be calculated as follows:

$$\mathrm{NDVI} = (R_{\mathrm{NIR}} - R_{\mathrm{red}})/(R_{\mathrm{NIR}} + R_{\mathrm{red}}) \tag{1}$$

$$\mathrm{EVI} = 2.5 \times (R_{\mathrm{NIR}} - R_{\mathrm{red}})/(R_{\mathrm{NIR}} + 6 \times R_{\mathrm{red}} - 7.5 \times R_{\mathrm{blue}} + 1) \tag{2}$$

$$\mathrm{SR} = R_{\mathrm{NIR}}/R_{\mathrm{red}} - 1 \tag{3}$$

where R_{NIR}, R_{red}, and R_{blue} are reflectance data in the NIR band 2, red band 1, and blue band 3, respectively.

3.4. *LUE estimation methods*

Two empirical statistical models were used to build relationship between LUE and MODIS reflectance data. One is a linear regression model. Stepwise selection method embedded in SPSS 13.0 software was used to select variables for the model, defining 0.05 and 0.10 as thresholds for adding and removing an independent variable, respectively. The other one is the partial least squares (PLS) regression. The PLS regression method has the ability to analyse data with noisy, collinear, and even incomplete variables in both dependent and

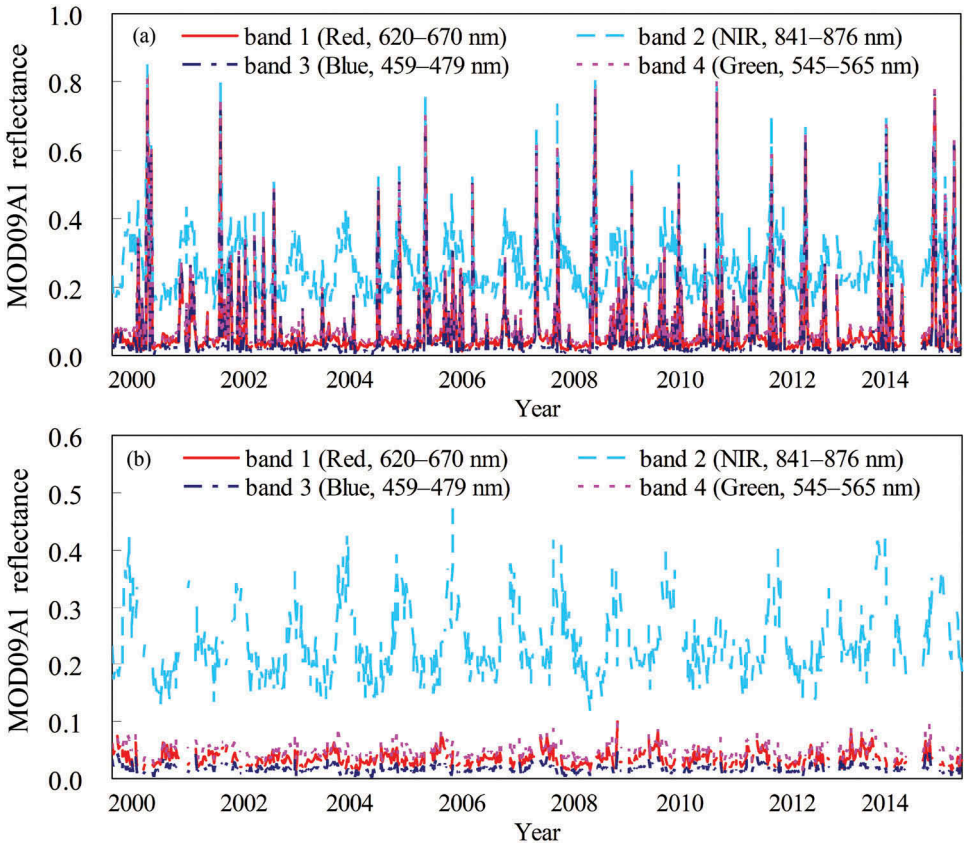

Figure 3. Time series of (a) raw MOD09A1 reflectance data and (b) values after removal of bad data for band 1 (red, 620–670 nm), band 2 (NIR, 841–876 nm), band 3 (blue, 459–479 nm), and band 4 (green, 545–565 nm).

independent data because a principal component analysis technique was involved in the PLS regression (Wold, Sjöström, and Eriksson 2001). The precision of the model parameters was also improved with increasing number of relevant variables and observations (Wold, Sjöström, and Eriksson 2001). A detailed description of the PLS regression is provided in Wold, Sjöström, and Eriksson (2001). The important step in using the PLS regression is to determine the number of components and the method for choosing the optimal number of components was described in Xu et al. (2011). The PLS-bootstrap algorithm was used to select variables, and details of the algorithm are presented in Lazraq, Cleroux, and Gauchi (2003). The PLS regression method was run using the Matlab R2010b software.

3.5. *LUE models for GPP estimation*

Three LUE models were used to estimate GPP and compared with measured GPP from EC. The three LUE models were also compared with each other in this study. The first LUE model (LUE-PAR) is that GPP is calculated by LUE estimates from this study multiplied by PAR (Equation (4)):

$$GPP_{LUE\text{-}PAR} = (PAR) \times (LUE) \tag{4}$$

The second LUE model is that the MOD17A2 model designed for the MODIS sensor aboard the Aqua and Terra platforms (Equation (5)). The details of the MOD17A2 model are presented in Running and Zhao (2015).

$$GPP_{MOD17A2} = \varepsilon_{max} \times T_{scalar} \times (VPD)_{scalar} \times (FPAR) \times (PAR) \tag{5}$$

where $GPP_{MOD17A2}$ is GPP estimates from the MOD17A2 model. ε_{max} is obtained from the biome properties look-up table and is constrained by using simple linear ramp functions of minimum air temperature (T_{scalar}) and vapour pressure deficit (VPD_{scalar}). Values of temperature, VPD, and PAR are obtained from the NASA's Global Modelling and Assimilation Office (GMAO/NASA) data set. FPAR is the fraction of PAR absorbed by the vegetation canopy. Satellite-derived FPAR product, which is directly qualified by the NDVI product, was used to calculate absorbed PAR.

The third LUE model is the EC-LUE model presented by Yuan et al. (2007) and has been successfully used in estimating GPP of Moso bamboo forest (Xu et al. 2013) (Equation (6)). The ε_{max} in the EC-LUE model is constrained by air temperature and moisture.

$$GPP_{EC\text{-}LUE} = \frac{G_{max} \times \varepsilon_{max} \times (\min(T_s, W_s) \times (FPAR) \times (PAR))}{\varepsilon_{max} \times (\min(T_s, W_s) \times (FPAR) \times (PAR)) + G_{max}} \tag{6}$$

where T_s and W_s are the downward-regulation scalars for the respective effects of air temperature and moisture on LUE of vegetation (Yuan et al. 2007). W_s is calculated as latent heat flux divided by net radiation (Yuan et al. 2010) and T_s is estimated based on the equation developed for the terrestrial ecosystem Model (Raich et al. 1991). G_{max} is the potential GPP. The meteorological inputs for the EC-LUE model, such as PAR, net radiation, and air temperature, are from the MERRA reanalysis data set at GMAO/NASA. The FPAR is calculated from NDVI data with a linear equation built by Myneni and Williams (1994). The latent heat flux is calculated using the remote-sensing-driven Penman–Monteith model (Mu et al. 2007).

3.6. *Statistic analysis*

The MODIS reflectance data, PAR, LUE, and GPP data set shown in Table 2 were used in this study. All data set were synthesized into 8-day average. Minimum and maximum values of measured/obtained parameters (such as LUE, GPP, and vegetation indices) along with

Table 2. Description of remote sensing data and biophysical parameters used in this study.

Dataset	Year	Temporal scale	Source
MOD09A1 band 1 ~ 7	2000–2014	8-day	ORNL DAAC
NDVI, EVI, SR	2000–2014	8-day	ORNL DAAC
PAR_{flux}	2011–2013	Daily	Anji EC flux tower
PAR_{MERRA}	2000–2014	Daily	GMAO/NASA
PAR_X	2011–2012	Daily	Xu, Du, Zhou, Mao et al. (2016)
LUE_{flux}	2011–2013 (n = 78)	Daily	Anji EC flux tower
GPP_{flux}	2011–2013 (n = 78)	Daily	Anji EC flux tower
$GPP_{MOD17A2}$	2000–2014	8-day	ORNL DAAC
$GPP_{EC\text{-}LUE}$	2003–2011	8-day	Xu et al. (2013)

Table 3. Minimum (Min) and maximum (Max) values of GPP_{flux}, LUE_{flux}, vegetation indices, and reflectance data (band 1 ~ band 7) along with standard deviation (Std).

	GPP_{flux}	LUE_{flux}	SR	NDVI	EVI	band 1	band 2	band 3	band 4	band 5	band 6	band 7
Min	1.69	0.04	2.09	0.51	0.23	0.01	0.14	0.01	0.03	0.16	0.12	0.05
Max	7.35	0.09	14.66	0.88	0.56	0.08	0.36	0.04	0.09	0.57	0.23	0.14
Std	1.42	0.01	2.59	0.08	0.08	0.01	0.05	0.01	0.01	0.06	0.03	0.02

standard deviation are shown in Table 3. The measured LUE and GPP from three years (2011, 2012, and 2013) with 78 available data were divided into two parts. The data set with sequence number (2, 6, 10…, 78) was used as an independent dataset (n = 20) for the validation of the prediction accuracy of the linear regression and PLS models. The remaining data set (n = 58) was used for building the linear regression and PLS models for the estimations of LUE. The goodness of fit of the linear regression and PLS models were measured by calculating the correlation coefficients (r), root mean squared error (RMSE), and relative RMSE (RMSEr) for the calibration and validation sets. The prediction accuracy of LUE models for estimating GPP were also evaluated by comparing GPP estimates with measured GPP from EC flux tower.

4. Results

4.1. *Relationships between reflectance data and LUE*

The correlation analysis between LUE of Moso bamboo forest and the reflectance data (Table 4) showed that the visible reflectance band has higher r with LUE than the NIR and mid-IR reflectance bands. The r of −0.38 ($p < 0.01$) between the red band 1 reflectance (620–670 nm) and LUE was the highest, implying that the red reflectance band is a good indicator for the estimation of LUE, followed by NDVI with r of 0.35 ($p < 0.01$) and SR with r of 0.33 ($p < 0.01$). The reflectances in the visible blue band 3 ($p < 0.05$) and the visible green band 1 ($p < 0.05$) had significantly negative correlation with LUE, whereas the NIR reflectance band 2 had the weakest relationships with LUE.

4.2. *LUE estimates from linear regression and PLS models*

Only reflectance data in band 1 was selected to build a linear regression model for the estimation of LUE based on a stepwise variable selection method using 58 sample data

Table 4. Correlation coefficients (r) between LUE_{flux} and reflectance data (band 1 ~ band 7) and between LUE_{flux} and vegetation indices.

Variable	r	p-value
Band 1 (620–670 nm)	−0.38	0.001
Band 2 (841–876 nm)	−0.05	0.698
Band 3 (459–479 nm)	−0.28	0.013
Band 4 (545–565 nm)	−0.25	0.026
Band 5 (1230–1250 nm)	−0.09	0.440
Band 6 (1628–1652 nm)	−0.13	0.265
Band 7 (2105–2155 nm)	−0.21	0.065
SR	0.33	0.004
NDVI	0.35	0.002
EVI	0.12	0.288

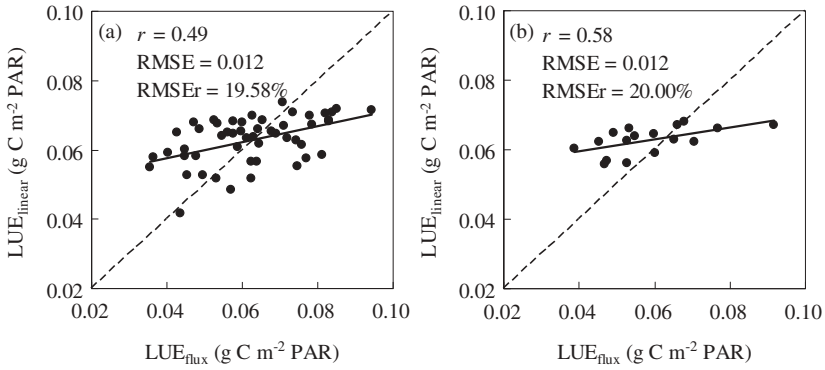

Figure 4. Comparison of predicted LUE (LUE_{linear}) from the linear regression model and measured LUE (LUE_{flux}), (a) calibration data set and (b) validation dataset. The 1:1 line is marked with a dashed line.

collected from 2011 to 2013. The linear regression equation (Equation (7)), which is significant at the level of 0.01, was used for estimating LUE.

$$LUE_{linear} = 0.081 - 0.497 \times R_{red} \tag{7}$$

The above equations yielded accuracy of $r = 0.49$ and RMSEr = 19.58% for the calibration data set and of $r = 0.58$ and RMSEr = 20.00% for the validation data set (Figure 4). The linear regression model has poor ability to predict high and low LUE values. The high LUE values were obviously underestimated, whereas the low LUE values were seriously overestimated.

Compared with stepwise selection method, three independent variables were selected from original 10 variables for the PLS regression model based on the PLS-bootstrap algorithm. The structure of the PLS equation (Equation (8), $p < 0.01$) used for estimating LUE is as follows:

$$LUE_{PLS} = -0.034 - 0.269 \times R_{NIR} + 0.712 \times R_{green} + 0.170 \times (NDVI) \tag{8}$$

where R_{green} is reflectance data in the green band 4.

The PLS regression model has the higher r and lower RMSEr values between the predicted LUE (LUE_{PLS}) and measured LUE from EC flux tower (LUE_{flux}) for both the calibration and the validation datasets than the linear regression model (Figure 5), implying that the PLS regression has better predictive ability for estimating LUE than the linear regression model. However, the same issue with the linear regression model happens in the PLS regression model. There exists the problem in slight overestimation of LUE_{flux} values lower than 0.05 g C m^{-2} PAR and underestimation of LUE_{flux} values greater than 0.07 g C m^{-2} PAR.

4.3. *Comparisons in GPP derived by different PAR estimates*

The resulting LUE_{PLS} is combined with PAR to calculate GPP. Effects of PAR from three different sources on GPP estimates are compared in this study (Table 5 and Figure 6). Compared with measured GPP from EC flux tower (GPP_{flux}), GPP estimates driven by the PAR_{flux} (GPP_{LPF}) have the highest accuracy with RMSE of 1.03 g C m^{-2} day^{-1} and RMSEr of 24.10% (Table 5 and Figure 6(a)). The RMSE and RMSEr of GPP estimates driven by the PAR_X

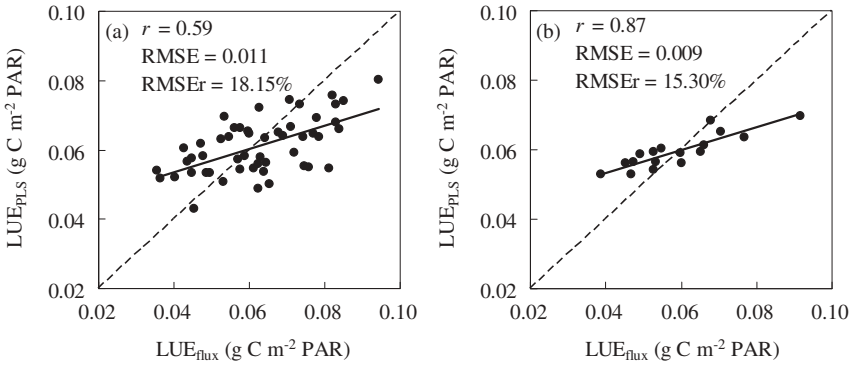

Figure 5. Comparison of predicted LUE (LUE_{PLS}) from the PLS regression model and measured LUE (LUE_{flux}), (a) calibration data set and (b) validation data set. The 1:1 line is marked with a dashed line.

Table 5. RMSE (g C m^{-2} day^{-1}) and RMSEr (%) of GPP estimates from the LUE-PAR model driven by different PAR data.

	2011		2012		2013		All data	
	RMSE	RMSEr	RMSE	RMSEr	RMSE	RMSEr	RMSE	RMSEr
GPP_{LPF}	0.83	17.26	1.22	39.46	1.29	31.15	1.03	24.10
GPP_{LPM}	1.15	23.97	2.20	71.41	1.58	38.24	1.63	38.04
GPP_{LPX}	0.87	18.10	1.40	45.26	/	/	1.10	25.21

(GPP_{LPX}) are comparable to those driven by the PAR_{flux} (Table 5 and Figure 6(b)), implying that the PAR_X with high spatial resolution and accuracy significantly reduced the uncertainty of the GPP estimates compared with GPP estimates driven by the PAR_{MERRA} (GPP_{LPM}). Compared to PAR_{flux} (Figure 6(a)) and PAR_X (Figure 6(b)), the PAR_{MERRA} results in obvious overestimation of GPP estimates (Figure 6(c)) and the absolute relative error (ARE) of GPP_{LPM} decreases as GPP_{flux} increases (Figure 7).

4.4. *Comparisons in GPP from different LUE models*

Compared with GPP_{flux} in 2011, GPP_{LPF} has the highest accuracy with RMSE of 0.83 g C m^{-2} day^{-1} and RMSEr of 17.26% (Table 5), which is comparable to GPP estimates derived from the EC-LUE model ($GPP_{EC\text{-}LUE}$) with RMSE of 0.86 g C m^{-2} day^{-1} and RMSEr of 17.96% (Xu et al. 2013). The MOD17A2 model has the poorest accuracy with RMSE of 1.57 g C m^{-2} day^{-1} and RMSEr of 32.95% (Xu et al. 2013). Results showed that the LUE-PAR model if high-quality PAR data available and the EC-LUE model exhibited the similar capabilities in simulating GPP of Moso bamboo forest and overall performed better than the MOD17A2 model.

GPP estimates from the three LUE models are also compared with each other (Figure 8). GPP estimates derived from the three LUE models have high correlation coefficients. GPP_{LPM} is slightly smaller than $GPP_{EC\text{-}LUE}$ with a bias of −0.78 g C m^{-2} day^{-1} (Figure 8(a)). GPP_{LPM} is obviously greater than $GPP_{MOD17A2}$ with a bias of 1.68 g C m^{-2} day^{-1} (Figure 8(b)). The relationship between the $GPP_{EC\text{-}LUE}$ and $GPP_{MOD17A2}$ is the strongest with r of 0.93 while the bias between them is the greatest with a bias of 2.53 g C m^{-2} day^{-1} (Figure 8(c)).

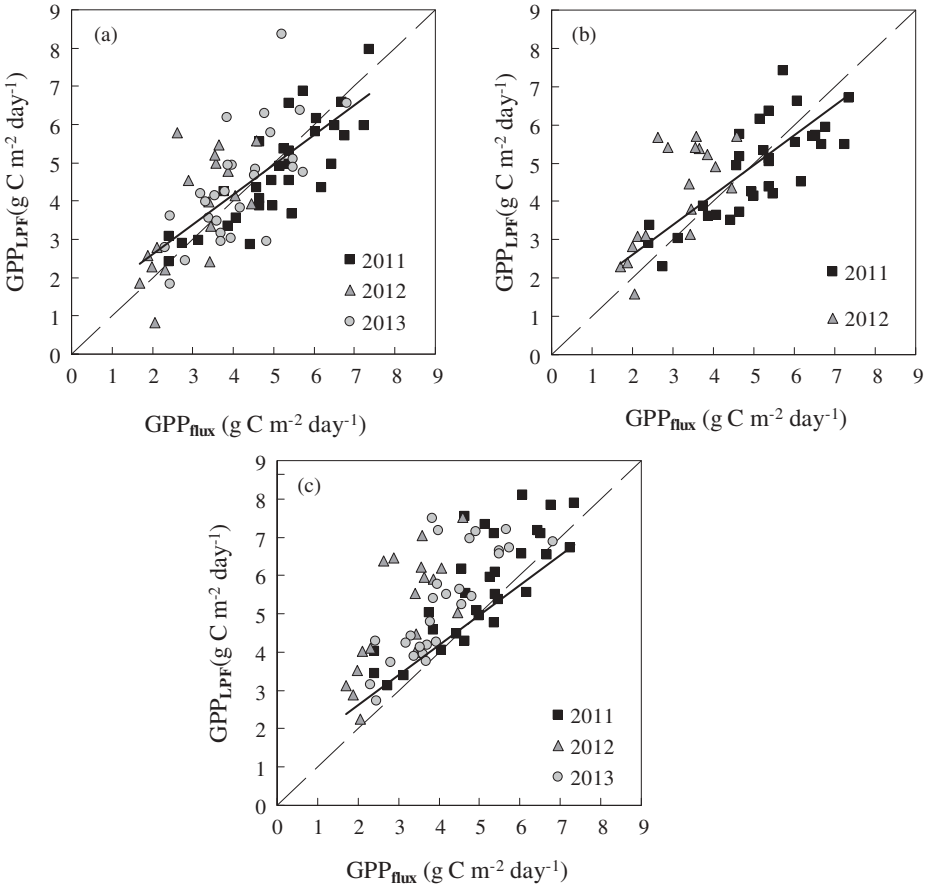

Figure 6. Comparison of predicted GPP and measured GPP (GPP_{flux}). The predicted GPP are from the LUE-PAR model driven by three different PAR sources, (a) PAR_{flux}, (b) PAR_X, and (c) PAR_{MERRA}, respectively. The 1:1 line is marked with a dashed line.

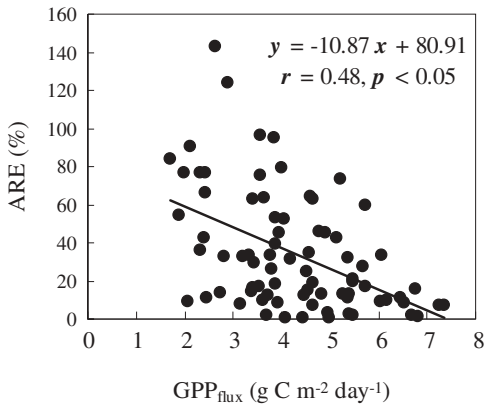

Figure 7. Changes in absolute relative error (ARE) of GPP_{LPM} as GPP_{flux} changes.

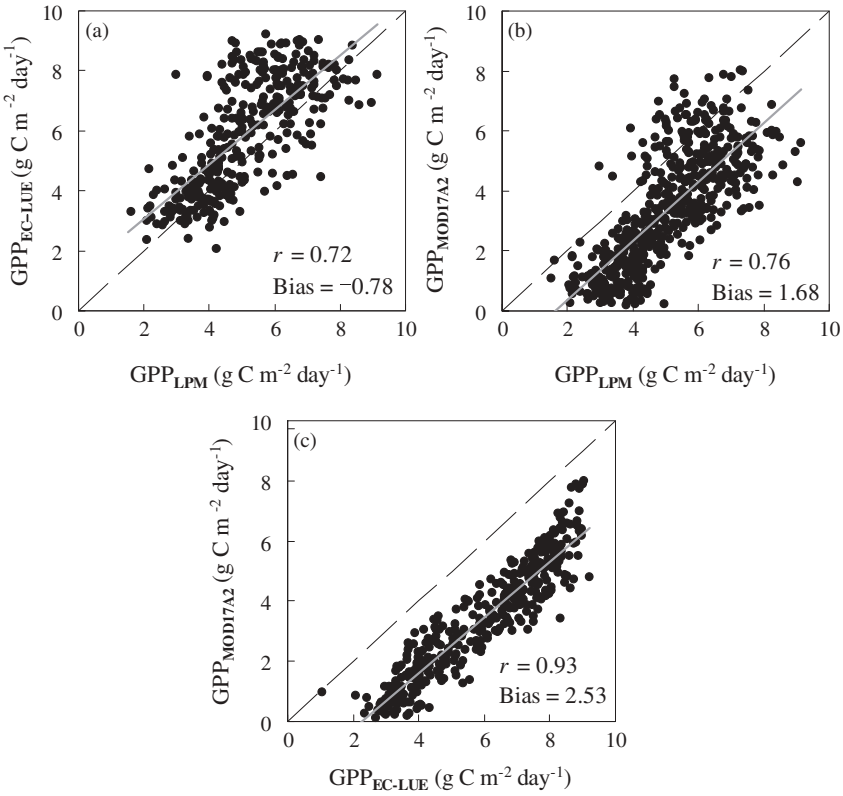

Figure 8. Comparisons of GPP estimates from three different LUE models, (a) GPP_{EC-LUE} vs. GPP_{LPM}, (b) $GPP_{MOD17A2}$ vs. GPP_{LPM}, and (c) $GPP_{MOD17A2}$ vs. GPP_{EC-LUE}.

Results showed that the EC-LUE model and the LUE-PAR model have similar performance but they are obviously different with the MOD17A2 model.

Time series of 8-day mean GPP estimates averaged by multi-years showed that the GPP_{LPM} is closer to GPP_{flux} than the other two LUE models with ARE smaller than 20% relative to GPP_{flux} in the period of DOY1 to DOY97 and DOY177 to DOY361 (Figures 9 and 10), which is attributed to counteract the underestimation in LUE_{PLS} to the overestimation of PAR_{MERRA} (Figure 10). However, it has overestimation problem with ARE far larger than 20% in the period of DOY 97 to DOY177 (Figures 9 and 10) due to superimposed effect of the overestimations of LUE_{PLS} and PAR_{MERRA} (Figure 10). GPP_{EC-LUE} overestimated GPP_{flux} with ARE larger than 20% in the period of DOY 97 to DOY361. $GPP_{MOD17A2}$ seriously underestimated GPP_{flux} with ARE larger than 20% in the period of DOY 1 to DOY97 and DOY 289 to DOY361 (Figure 9).

5. Discussion

5.1. *Factors effect on accuracy of LUE estimates*

Correlation coefficient analysis showed that LUE has the strongest relationship with red band. Previous study showed that the photochemical reactance index calculated using

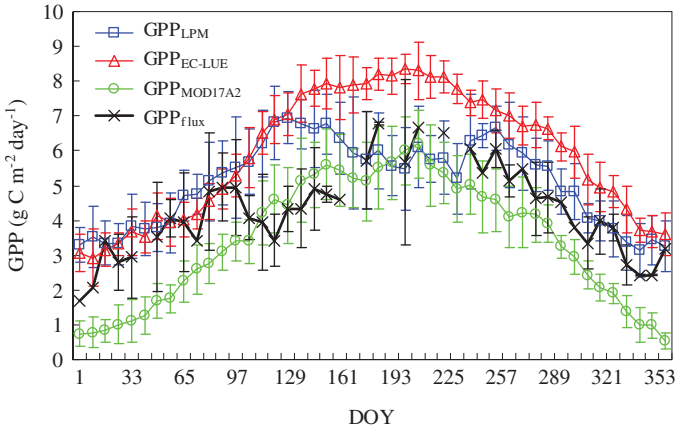

Figure 9. Time series of 8-day mean GPP estimates, GPP $_{LPM}$ from 2000 to 2014, GPP$_{EC-LUE}$ from 2003 to 2011, GPP$_{MOD17A2}$ from 2000 to 2014, and GPP$_{flux}$ from 2011 to 2013. Vertical bar is ±1 standard deviation.

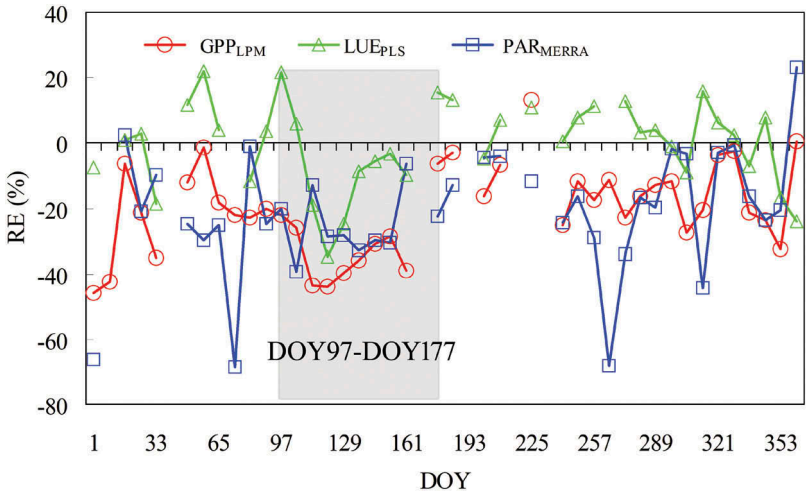

Figure 10. Time series of relative error (RE) for GPP$_{LPM}$, LUE$_{PLS}$, and PAR$_{MERRA}$ averaged from 2011 to 2013. Positive RE means underestimation; negative RE means overestimation.

red band was significantly related to LUE (Table 4), implying that the red band is an important reflectance region for LUE estimation (Goerner, Reichstein, and Rambal 2009). The magnitude of LUE is highly related to the chlorophyll content in forest canopy (Wu et al. 2009). The reflectances in blue and red bands are affected by the chlorophyll content (Datt 1999). Therefore, the high negative relationships between LUE and visible reflectance bands are attributed to the strong absorption by chlorophyll content in the visible blue and red regions (Gitelson et al. 2005; Peng et al. 2011).

Except for chlorophyll content, the reflectance data of MODIS bands are affected by many other factors, such as leaf area index, soil background, cloud, and atmospheric matter, which will reduce the correlations between LUE and reflectance bands. The

source area of LUE_{flux} represents the footprint area (Chen et al. 2011), which is different with the pixel area of MODIS 09A1. The scale problem also causes reduction in correlations between LUE and reflectance bands.

The PLS regression model performed better than the linear regression model (Figures 4 and 5). The main difference between the linear regression model and the PLS regression model is the selected independent variables resulting from the different variable selection strategies. The PLS-bootstrap algorithm has advantages in eliminating collinearity among reflectance in bands and solving the effect of noisy reflectance data on model parameters (Wold, Sjöström, and Eriksson 2001; Lazraq, Cleroux, and Gauchi 2003). In this study, the band 2, band 4, and NDVI were selected as independent variables, although there are high correlations between each other. The critical problem in LUE estimates is the overestimation in low LUE values and the underestimation in high LUE values. In this study, only MODIS reflectance data were used to explain LUE using the empirical statistical models. Many other factors closely related to LUE were not considered into the models for estimation of LUE, which is one of factors resulting in uncertainty of LUE estimates. The climatic conditions have close relationship with variability in LUE at finer temporal scales (Running and Zhao 2015; Wu et al. 2012). Wu et al. (2012) proposed a new algorithm that incorporates the temperature for estimating monthly forest LUE based on MODIS imagery. The algorithm performed better than models including only EVI (Wu et al. 2012). Considering the impacts of solar radiation partitioning increased accuracy for modelling crop GPP on a daily or shorter basis because canopy LUE could vary with illumination conditions (Xin et al. 2016).

5.2. *Effect of PAR on GPP estimates*

The impacts of different PAR products on GPP estimates have been tested. Results from this study are consistent with other researches, which showed the errors of the PAR products significantly impacted the accuracy of the GPP estimates and the GPP estimates derived from satellite-based PAR products have the low errors compared with GPP estimates derived from the PAR_{flux} (Cai et al. 2014; Li, Ju et al. 2015). The PAR_{MERRA} product tended to overestimate radiation relative to PAR_{flux} and further resulted in overestimating GPP (Cai et al. 2014; Xu, Du, Zhou, Mao et al. 2016). There is huge difference in spatial resolution between satellite-based PAR_X product and PAR_{MERRA} product. The PAR_X derived from MODIS atmospheric products has higher spatial resolution than the PAR_{MERRA} product. The 1 km spatial resolution of PAR_X is closer to the footprint area of EC flux tower than the PAR_{MERRA} product, which may be the main reason for low errors in GPP estimates derived from the PAR_X. Therefore, high-resolution satellite-derived radiation products were suggested to be used for GPP estimation (Cai et al. 2014; Jin et al. 2015).

5.3. *Comparisons of LUE models*

Compared with GPP_{flux}, GPP estimates from the three LUE models have significantly different. The model inputs and model parameters are the main factors resulting in the differences among the three LUE models. The LUE-PAR model proposed in this study has the highest accuracy but tended to overestimate GPP from DOY 97 (beginning of April) to DOY177 (ending of June) (Figures 9 and 10). The LUE-PAR model overestimates the GPP in this period due to overestimations in both of LUE_{PLS} and PAR_{MERRA} (Figure 10). The reasons

for overestimation of LUE in this period derived from remote-sensing data are that Moso bamboo forest in this period of DOY 97 to DOY177 has complicated phenological characteristics, such as changing leaf, the flushing of new shoots, and new leaf spread. These phenological characteristics are significantly different between the on-year and off-year. The amount of fallen leaves in the Moso bamboo forests change annually (Li et al. 1998). Two-year-old leaves in the off-year are dropped in April and are replaced by one-year-old leaves (Li et al. 1998), but this phenomenon does not occur in an on-year. Two-year-old leaves of old bamboo in the on-year turn yellow after the flushing of new shoots in March, because the growth of bamboo shoots consumes considerable quantities of carbohydrate and nutrients (Qiu 1984; Hu 2011). The rate of photosynthesis of one-year-old leaves is up to 3 times higher than that of two-year-old leaves (Huang et al. 1989; Kleinhenz and Midmore 2001). These complicated phenological characteristics not only cause greater differences in LUE and GPP but also in remote-sensing data. Therefore, there may be different responses of LUE and GPP values to remote-sensing data between the on-year and off-year because of different phenological characteristics between the on-year and off-year, which may affect the accurate estimation of LUE and GPP during DOY97 to DOY177.

The EC-LUE model driven by PAR_{MERRA} tended to overestimate GPP (Figure 9), which is consistent to another study using the EC-LUE model (Cai et al. 2014). The main reason for the overestimation in GPP derived from the EC-LUE model is due to overestimation in PAR_{MERRA} relative to PAR_{flux} (Cai et al. 2014; Xu, Du, Zhou, Mao et al. 2016). Previous researches showed that there exists obvious problem in underestimation of MODIS LAI product during the period from DOY1 to DOY97 (Xu, Du, Zhou, and Li 2016; Li et al. 2017; Mao et al. 2017), which implies underestimation in FPAR derived from MODIS NDVI product during the same period. Therefore, the high accuracy of GPP estimates derived from the EC-LUE model during the period from DOY1 to DOY97 (Figure 9) because the effect of FPAR underestimation on GPP estimates offsets by the effect of PAR_{MERRA} overestimation on GPP estimates.

GPP calculated from the MOD17A2 model had greater error than those from the LUE_{PLS}_PAR_{MERRA} model and the EC-LUE model (Table 5 and Figure 9), which is consistent with previous studies using the EC-LUE model (Xu et al. 2013) and the other LUE models (Wu et al. 2010; Jahan and Gan 2013; Gao et al. 2014; Wagle et al. 2016). The MOD17A2 model tended to underestimate GPP of Moso bamboo forest with the estimates being 32.95% (Xu et al. 2013) less than GPP_{flux}, which is comparable to previous studies for other species (Coops et al. 2007; Sjöström et al. 2011; Wang et al. 2015). For example, GPP estimates of a Douglas-fir forest stand based on the MOD17A2 model were highly correlated with the GPP_{flux} but these estimates were biased with the estimates being 30% less than the GPP_{flux} (Coops et al. 2007). The main reason for underestimation in GPP estimates from the MOD17A2 model is uncertainty in ε_{max}. The ε_{max} for mixed forest (1.05 g C m^{-2} day^{-1} MJ^{-1}) was used for calculating GPP of Moso bamboo forest, which is lower than the ε_{max} (2.08 g C m^{-2} day^{-1} MJ^{-1}) of Moso bamboo forest calibrated with EC measurements (Xu et al. 2013; Running and Zhao 2015). The ε_{max} for grasslands and deciduous forests were also found to be underestimated in previous study and refinements of MOD17 ε_{max} may be beneficial for GPP estimation (Yang et al. 2007). $GPP_{MOD17A2}$ was highly related to $GPP_{EC\text{-}LUE}$; however, $GPP_{MOD17A2}$ was obviously lower than $GPP_{EC\text{-}LUE}$. The reason for that is because ε_{max} for the MOD17A2 model is lower than ε_{max} for the EC-LUE model (Xu et al. 2013; Running and Zhao 2015).

6. Conclusions

This study presented a superior approach for estimating GPP of Moso bamboo forest based on the assumption of high relationships between LUE and MODIS reflectance data. Correlation analysis showed that MODIS reflectance data in visible light regions were good predictors for estimation of LUE. The PLS model has stronger capability in predicting LUE than the linear regression model based on the MODIS reflectance data because the PLS model can solve the collinear problem between independent variables. However, the underestimation in high LUE values and overestimation in low LUE values are still unsolved by the PLS model. Compared with observed PAR, the PAR derived from a solar radiation model driven by MODIS atmospheric products with 1 km spatial resolution is more useful for estimating GPP than the MERRA radiation product, implying PAR product with high spatial resolution has the potential to improving GPP estimation. The LUE-PAR model, which means GPP is calculated by the product of LUE and PAR, has the highest accuracy than the EC-LUE model and the MOD17A2 model, which is a promising and simple way to estimate GPP of Moso bamboo forest. The GPP estimates derived from the EC-LUE model obviously overestimated the GPP because of overestimation in the MERRA radiation product. The GPP estimates derived from the MOD17A2 model obviously underestimated the GPP due to underestimation in ε_{max} of Moso bamboo forest. Therefore, Moso bamboo forest, as a special forest type, is suggested to be treated as a new land-cover class and included into land-cover product (MOD12). A species-specific ε_{max} was necessary to be selected and used in the MOD17A2 model for estimating GPP of Moso bamboo forest.

Acknowledgements

This research was supported by the National Natural Science Foundation (Grant Nos. 31500520, 31370637, and 31670644) and Natural Science Foundation of Zhejiang Province (Grant No. LQ15C160003).

Disclosure statement

No potential conflict of interest was reported by the authors.

Funding

This work was supported by the National Natural Science Foundation of China [Grant Nos. 31500520, 31370637, and 31670644] and Natural Science Foundation of Zhejiang Province [Grant No. LQ15C160003].

References

Cai, W., W. Yuan, S. Liang, X. Zhang, W. Dong, J. Xia, Y. Fu, Y. Chen, D. Liu, and Q. Zhang. 2014. "Improved Estimations of Gross Primary Production Using Satellite-Derived Photosynthetically Active Radiation." *Journal of Geophysical Research Biogeosciences* 119 (1): 110–123. doi:10.1002/2013JG002456.

Chen, B., N. C. Coops, D. Fu, H. A. Margolis, B. D. Amiro, A. G. Barr, T. A. Black, M. A. Arain, P. A. Bourque, and L. B. Flanagan. 2011. "Assessing Eddy-Covariance Flux Tower Location Bias across

the Fluxnet-Canada Research Network Based on Remote Sensing and Footprint Modelling." *Agricultural & Forest Meteorology* 151 (1): 87–100. doi:10.1016/j.agrformet.2010.09.005.

Chen, X. G., X. Q. Zhang, Y. P. Zhang, T. Booth, and X. H. He. 2009. "Changes of Carbon Stocks in Bamboo Stands in China during 100 Years." *Forest Ecology & Management* 258 (7): 1489–1496. doi:10.1016/j.foreco.2009.06.051.

Cheng, Y. B., Q. Zhang, A. I. Lyapustin, Y. Wang, and E. M. Middleton. 2014. "Impacts of Light Use Efficiency and fPAR Parameterization on Gross Primary Production Modeling." *Agricultural & Forest Meteorology* 189–190 (6): 187–197. doi:10.1016/j.agrformet.2014.01.006.

Coops, N. C., T. A. Black, R. S. Jassal, J. A. Trofymow, and M. Kai. 2007. "Comparison of MODIS, Eddy Covariance Determined and Physiologically Modelled Gross Primary Production (GPP) in a Douglas-Fir Forest Stand." *Remote Sensing of Environment* 107 (3): 385–401. doi:10.1016/j.rse.2006.09.010.

Datt, B. 1999. "A New Reflectance Index for Remote Sensing of Chlorophyll Content in Higher Plants: Tests Using Eucalyptus Leaves." *Journal of Plant Physiology* 154 (1): 30–36. doi:10.1016/S0176-1617(99)80314-9.

Gamon, J. A., L. Serrano, and J. S. Surfus. 1997. "The Photochemical Reflectance Index: An Optical Indicator of Photosynthetic Radiation Use Efficiency across Species, Functional Types, and Nutrient Levels." *Oecologia* 112 (4): 492–501. doi:10.1007/s004420050337.

Gao, Y., G. Yu, H. Yan, X. Zhu, S. Li, Q. Wang, J. Zhang, Y. Wang, Y. Li, and L. Zhao. 2014. "A MODIS-based Photosynthetic Capacity Model to Estimate Gross Primary Production in Northern China and the Tibetan Plateau." *Remote Sensing of Environment* 148 (5): 108–118. doi:10.1016/j.rse.2014.03.006.

Gitelson, A. A., A. Viña, S. B. Verma, D. C. Rundquist, T. J. Arkebauer, G. Keydan, B. Leavitt, V. Ciganda, G. G. Burba, and A. E. Suyker. 2006. "Relationship between Gross Primary Production and Chlorophyll Content in Crops: Implication for the Synoptic Monitoring of Vegetation Productivity." *Journal of Geophysical Research Atmospheres* 111 (D8): 854–871. doi:10.1029/2005JD006017.

Gitelson, A. A., A. Viña, V. Ciganda, D. C. Rundquist, and T. J. Arkebauer. 2005. "Remote Estimation of Canopy Chlorophyll Content in Crops." *Geophysical Research Letters* 32 (8): 93–114. doi:10.1029/2005GL022688.

Gitelson, A. A., Y. Peng, T. J. Arkebauer, and J. Schepers. 2014. "Relationships between Gross Primary Production, Green LAI, and Canopy Chlorophyll Content in Maize: Implications for Remote Sensing of Primary Production." *Remote Sensing of Environment* 144 (4): 65–72. doi:10.1016/j.rse.2014.01.004.

Goerner, A., M. Reichstein, and S. Rambal. 2009. "Tracking Seasonal Drought Effects on Ecosystem Light Use Efficiency with Satellite-Based PRI in a Mediterranean Forest." *Remote Sensing of Environment* 113 (5): 1101–1111. doi:10.1016/j.rse.2009.02.001.

Groenendijk, M., A. J. Dolman, M. K. V. D. Molen, R. Leuning, A. Arneth, N. Delpierre, J. H. C. Gash, A. Lindroth, A. D. Richardson, and H. Verbeeck. 2011. "Assessing Parameter Variability in a Photosynthesis Model within and between Plant Functional Types Using Global Fluxnet Eddy Covariance Data." *Agricultural & Forest Meteorology* 151 (1): 22–38. doi:10.1016/j.agrformet.2010.08.013.

Hember, R. A., N. C. Coops, T. A. Black, and R. D. Guy. 2010. "Simulating Gross Primary Production Across a Chronosequence of Coastal Douglas-fir Forest Stands with a Production Efficiency Model." *Agricultural and Forest Meteorology* 150 (2): 238–253. doi: 10.1016/j.agrformet.2009.11.004.

Hilker, T., N. C. Coops, M. A. Wulder, T. A. Black, and R. D. Guy. 2008. "The Use of Remote Sensing in Light Use Efficiency Based Models of Gross Primary Production: A Review of Current Status and Future Requirements." *Science of the Total Environment* 404 (2–3): 411. doi:10.1016/j.scitotenv.2007.11.007.

Hu, Y. B. 2011. Effects of Fertilizations on Leaf Characteristics and Photosynthesis Character during the Shoot Period to Deciduous Period of Phyllostarchys Pubescens. Hangzhou: Zhejiang A&F University. [in Chinese].

Huang, Q., D. Yang, A. Gao, Y. Shen, G. Qiu, S. Long, C. Beadle, D. Hall, and J. Scurlock. 1989. "Research on Photosynthesis of Bamboo." *Bamboo Research (China)* 8 (2): 8–18. [in Chinese].

Jahan, N., and T. Y. Gan. 2013. "Developing a Gross Primary Production Model for Coniferous Forests of Northeastern USA from MODIS Data." *International Journal of Applied Earth Observation & Geoinformation* 25 (4): 11–20. doi:10.1016/j.jag.2013.03.006.

Jin, C., X. Xiao, P. Wagle, T. Griffis, J. Dong, C. Wu, Y. Qin, and D. R. Cook. 2015. "Effects of In-Situ and Reanalysis Climate Data on Estimation of Cropland Gross Primary Production Using the Vegetation Photosynthesis Model." *Agricultural & Forest Meteorology* 213 (25): 240–250. doi:10.1016/j.agrformet.2015.07.003.

Keenan, T. F., I. Baker, A. Barr, P. Ciais, K. Davis, M. Dietze, D. Dragoni, C. M. Gough, R. Grant, and D. Hollinger. 2012. "Terrestrial Biosphere Model Performance for Inter-Annual Variability of Land-Atmosphere CO2 Exchange." *Global Change Biology* 18 (6): 1971–1987. doi:10.1111/j.1365-2486.2012.02678.x.

Kleinhenz, V., and D. J. Midmore. 2001. "Aspects of Bamboo Agronomy." *Advances in Agronomy* 74 (1): 99–153. doi:10.1016/S0065-2113(01)74032-1.

Komatsu, H., Y. Onozawa, T. Kume, K. Tsuruta, T. Kumagai, Y. Shinohara, and K. Otsuki. 2010. "Stand-scale Transpiration Estimates in a Moso Bamboo Forest: II. Comparison with Coniferous Forests." *Forest Ecology And Management* 260 (8): 1295–1302. doi:10.1016/j.foreco.2010.07.012.

Lasslop, G., M. Reichstein, D. Papale, A. D. Richardson, A. Arneth, A. Barr, P. C. Stoy, and G. Wohlfahrt. 2010. "Separation of Net Ecosystem Exchange into Assimilation and Respiration using a Light Response Curve Approach: Critical Issues and Global Evaluation." *Global Change Biology* 16 (1): 187–208. doi: 10.1111/j.1365-2486.2009.02041.x.

Lazraq, A., R. Cleroux, and J. P. Gauchi. 2003. "Selecting Both Latent and Explanatory Variables in the PLS1 Regression Model." *Chemometrics & Intelligent Laboratory Systems* 66 (2): 117–126. doi:10.1016/S0169-7439(03)00027-3.

Li, D., W. Ju, D. Lu, Y. Zhou, and H. Wang. 2015. "Impact of Estimated Solar Radiation on Gross Primary Productivity Simulation in Subtropical Plantation in Southeast China." *Solar Energy* 120 (120): 175–186. doi:10.1016/j.solener.2015.07.033.

Li, P., G. Zhou, H. Du, D. Lu, L. Mo, X. Xu, Y. Shi, and Y. Zhou. 2015. "Current and Potential Carbon Stocks in Moso Bamboo Forests in China." *Journal of Environmental Management* 156: 89–96. doi:10.1016/j.jenvman.2015.03.030.

Li, R., M. J. A. Werger, H. J. During, and Z. C. Zhong. 1998. "Biennial Variation in Production of New Shoots in Groves of the Giant Bamboo Phyllostachys Pubescens in Sichuan, China." *Plant Ecology* 135 (1): 103–112. doi:10.1023/A:1009761428401.

Li, X., F. Mao, H. Du, G. Zhou, X. Xu, N. Han, S. Sun, G. Gao, and L. Chen. 2017. "Assimilating Leaf Area Index of Three Typical Types of Subtropical Forest in China from MODIS Time Series Data Based on the Integrated Ensemble Kalman Filter and PROSAIL Model." *Isprs Journal of Photogrammetry & Remote Sensing* 126: 68–78. doi:10.1016/j.isprsjprs.2017.02.002.

Li, Y., J. Zhang, S. X. Chang, P. Jiang, G. Zhou, S. Fu, E. Yan, J. Wu, and L. Lin. 2013. "Long-Term Intensive Management Effects on Soil Organic Carbon Pools and Chemical Composition in Moso Bamboo (Phyllostachys Pubescens) Forests in Subtropical China." *Forest Ecology & Management* 303 (5): 121–130. doi:10.1016/j.foreco.2013.04.021.

Lobovikov, M., S. Paudel, M. Piazza, H. Ren, and J. Wu. 2007. "World Bamboo Resources. A Thematic Study Prepared in the Framework of the Global Forest Resources Assessment 2005." *Non-Wood Forest Products (FAO)*.

Lou, Y. P., Y. X. Li, K. Buckingham, G. Henley, and G. M. Zhou. 2010. "Bamboo and Climate Change Mitigation." Technical Report No. 32, Beijing: International Network for Bamboo and Rattan (INBAR).

Mao, F., X. Li, H. Du, G. Zhou, N. Han, X. Xu, Y. Liu, L. Chen, and L. Cui. 2017. "Comparison of Two Data Assimilation Methods for Improving MODIS LAI Time Series for Bamboo Forests." *Remote Sensing* 9 (5): 401. doi:10.3390/rs9050401.

Mu, Q., F. A. Heinsch, M. Zhao, and S. W. Running. 2007. "Development of a Global Evapotranspiration Algorithm Based on MODIS and Global Meteorology Data." *Remote Sensing of Environment* 111 (4): 519–536. doi:10.1016/j.rse.2007.04.015.

Myneni, R. B., D. L. Williams, R. B. Myneni, and D. L. Williams. 1994. "On the Relationship between fAPAR and NDVI." *Remote Sensing of Environment* 49 (3): 200–211. doi:10.1016/0034-4257(94)90016-7.

Papale, D., M. Reichstein, M. Aubinet, E. Canfora, C. Bernhofer, W. Kutsch, B. Longdoz, S. Rambal, R. Valentini, and T. Vesala. 2006. "Towards a Standardized Processing of Net Ecosystem Exchange Measured with Eddy Covariance Technique: Algorithms and Uncertainty Estimation." *Biogeosciences* 3 (4): 571–583. doi:10.5194/bg-3-571-2006.

Peng, Y., A. A. Gitelson, G. Keydan, D. C. Rundquist, and W. Moses. 2011. "Remote Estimation of Gross Primary Production in Maize and Support for a New Paradigm Based on Total Crop Chlorophyll Content." *Remote Sensing of Environment* 115 (4): 978–989. doi:10.1016/j.rse.2010.12.001.

Potter, C. S., J. T. Randerson, C. B. Field, P. A. Matson, P. M. Vitousek, H. A. Mooney, and S. A. Klooster. 1993. "Terrestrial Ecosystem Production: A Process Model Based on Global Satellite and Surface Data." *Global Biogeochemical Cycles* 7 (4): 811–841. doi:10.1029/93GB02725.

Qiu, F. 1984. "The On-Year and Off-Year of Phyllostachys Pubescens Forests and Their Control." *Journal of Bamboo Research* 3: 62–69. [in Chinese].

Raich, J., E. Rastetter, J. Melillo, D. Kicklighter, P. Steudler, B. Peterson, A. Grace, B. Moore, and C. Vorosmarty. 1991. "Potential Net Primary Productivity in South America: Application of a Global Model." *Ecological Applications* 1 (4): 399–429. doi:10.2307/1941899.

Running, S., and M. Zhao. 2015. User's Guide Daily GPP and Annual NPP (MOD17A2/A3) Products NASA Earth Observing System MODIS Land Algorithm. Missoula: University of Montana.

Sjöström, M., J. Ardö, A. Arneth, N. Boulain, B. Cappelaere, L. Eklundh, A. De Grandcourt, W. L. Kutsch, L. Merbold, and Y. Nouvellon. 2011. "Exploring the Potential of MODIS EVI for Modeling Gross Primary Production across African Ecosystems." *Remote Sensing of Environment* 115 (4): 1081–1089. doi:10.1016/j.rse.2010.12.013.

Turner, D. P., S. Urbanski, D. Bremer, S. C. Wofsy, T. Meyers, S. T. Gower, and M. Gregory. 2003. "A Cross-Biome Comparison of Daily Light Use Efficiency for Gross Primary Production." *Global Change Biology* 9 (3): 383–395. doi:10.1046/j.1365-2486.2003.00573.x.

Wagle, P., P. H. Gowda, X. Xiao, and K. Anup. 2016. "Parameterizing Ecosystem Light Use Efficiency and Water Use Efficiency to Estimate Maize Gross Primary Production and Evapotranspiration Using MODIS EVI." *Agricultural and Forest Meteorology* 222: 87–97. doi:10.1016/j.agrformet.2016.03.009.

Wang, H., G. Jia, C. Fu, J. Feng, T. Zhao, and Z. Ma. 2010. "Deriving Maximal Light Use Efficiency from Coordinated Flux Measurements and Satellite Data for Regional Gross Primary Production Modeling." *Remote Sensing of Environment* 114 (10): 2248–2258. doi:10.1016/j.rse.2010.05.001.

Wang, S., K. Huang, H. Yan, H. Yan, L. Zhou, H. Wang, J. Zhang, J. Yan, L. Zhao, and Y. Wang. 2015. "Improving the Light Use Efficiency Model for Simulating Terrestrial Vegetation Gross Primary Production by the Inclusion of Diffuse Radiation across Ecosystems in China." *Ecological Complexity* 23: 1–13. doi:10.1016/j.ecocom.2015.04.004.

Wold, S., M. Sjöström, and L. Eriksson. 2001. "PLS-regression: A Basic Tool of Chemometrics." *Chemometrics and Intelligent Laboratory Systems* 58 (2): 109–130. doi:10.1016/S0169-7439(01)00155-1.

Wu, C., J. M. Chen, A. R. Desai, D. Y. Hollinger, M. A. Arain, H. A. Margolis, C. M. Gough, and R. M. Staebler. 2012. "Remote Sensing of Canopy Light Use Efficiency in Temperate and Boreal Forests of North America Using MODIS Imagery." *Remote Sensing of Environment* 118: 60–72. doi:10.1016/j.rse.2011.11.012.

Wu, C., J. W. Munger, Z. Niu, and D. Kuang. 2010. "Comparison of Multiple Models for Estimating Gross Primary Production Using MODIS and Eddy Covariance Data in Harvard Forest." *Remote Sensing of Environment* 114 (12): 2925–2939. doi:10.1016/j.rse.2010.07.012.

Wu, C., Z. Niu, Q. Tang, W. Huang, B. Rivard, and J. Feng. 2009. "Remote Estimation of Gross Primary Production in Wheat Using Chlorophyll-Related Vegetation Indices." *Agricultural and Forest Meteorology* 149 (6): 1015–1021. doi:10.1016/j.agrformet.2008.12.007.

Xiao, X., D. Hollinger, J. Aber, M. Goltz, E. A. Davidson, Q. Zhang, and B. Moore. 2004. "Satellite-Based Modeling of Gross Primary Production in an Evergreen Needleleaf Forest." *Remote Sensing of Environment* 89 (4): 519–534. doi:10.1016/j.rse.2003.11.008.

Xin, Q., M. Broich, A. E. Suyker, L. Yu, and P. Gong. 2015. "Multi-Scale Evaluation of Light Use Efficiency in MODIS Gross Primary Productivity for Croplands in the Midwestern United States." *Agricultural and Forest Meteorology* 201: 111–119. doi:10.1016/j.agrformet.2014.11.004.

Xin, Q., P. Gong, A. E. Suyker, and Y. Si. 2016. "Effects of the Partitioning of Diffuse and Direct Solar Radiation on Satellite-Based Modeling of Crop Gross Primary Production." *International Journal of Applied Earth Observation and Geoinformation* 50: 51–63. doi:10.1016/j.jag.2016.03.002.

Xu, X., G. Zhou, S. Liu, H. Du, L. Mo, Y. Shi, H. Jiang, Y. Zhou, and E. Liu. 2013. "Implications of Ice Storm Damages on the Water and Carbon Cycle of Bamboo Forests in Southeastern China." *Agricultural and Forest Meteorology* 177: 35–45. doi:10.1016/j.agrformet.2013.04.005.

Xu, X., H. Du, G. Zhou, F. Mao, P. Li, W. Fan, and D. Zhu. 2016. "A Method for Daily Global Solar Radiation Estimation from Two Instantaneous Values Using MODIS Atmospheric Products." *Energy* 111: 117–125. doi:10.1016/j.energy.2016.05.095.

Xu, X., H. Du, G. Zhou, H. Ge, Y. Shi, Y. Zhou, W. Fan, and W. Fan. 2011. "Estimation of Aboveground Carbon Stock of Moso Bamboo (Phyllostachys Heterocycla Var. Pubescens) Forest with a Landsat Thematic Mapper Image." *International Journal of Remote Sensing* 32 (5): 1431–1448. doi:10.1080/01431160903551389.

Xu, X., H. Du, G. Zhou, and P. Li. 2016. "Method for Improvement of MODIS Leaf Area Index Products Based on Pixel-To-Pixel Correlations." *European Journal of Remote Sensing* 49 (1): 57–72. doi:10.5721/EuJRS20164904.

Yang, F., K. Ichii, M. A. White, H. Hashimoto, A. R. Michaelis, P. Votava, A.-X. Zhu, A. Huete, S. W. Running, and R. R. Nemani. 2007. "Developing a Continental-Scale Measure of Gross Primary Production by Combining MODIS and AmeriFlux Data through Support Vector Machine Approach." *Remote Sensing of Environment* 110 (1): 109–122. doi:10.1016/j.rse.2007.02.016.

Yen, T. M. 2015. "Comparing Aboveground Structure and Aboveground Carbon Storage of an Age Series of Moso Bamboo Forests Subjected to Different Management Strategies." *Journal of Forest Research* 20 (1): 1–8. doi:10.1007/s10310-014-0455-0.

Yen, T. M. 2016. "Culm Height Development, Biomass Accumulation and Carbon Storage in an Initial Growth Stage for a Fast-Growing Moso Bamboo (Phyllostachy Pubescens)." *Botanical Studies* 57 (1): 10. doi:10.1186/s40529-016-0126-x.

Yen, T. M., and J.-S. Lee. 2011. "Comparing Aboveground Carbon Sequestration between Moso Bamboo (Phyllostachys Heterocycla) and China Fir (Cunninghamia Lanceolata) Forests Based on the Allometric Model." *Forest Ecology and Management* 261 (6): 995–1002. doi:10.1016/j.foreco.2010.12.015.

Yuan, W., S. Liu, G. Yu, J.-M. Bonnefond, J. Chen, K. Davis, A. R. Desai, A. H. Goldstein, D. Gianelle, and F. Rossi. 2010. "Global Estimates of Evapotranspiration and Gross Primary Production Based on MODIS and Global Meteorology Data." *Remote Sensing of Environment* 114 (7): 1416–1431. doi:10.1016/j.rse.2010.01.022.

Yuan, W., S. Liu, G. Zhou, G. Zhou, L. L. Tieszen, D. Baldocchi, C. Bernhofer, H. Gholz, A. H. Goldstein, and M. L. Goulden. 2007. "Deriving a Light Use Efficiency Model from Eddy Covariance Flux Data for Predicting Daily Gross Primary Production across Biomes." *Agricultural and Forest Meteorology* 143 (3): 189–207. doi:10.1016/j.agrformet.2006.12.001.

Yuan, W., W. Cai, J. Xia, J. Chen, S. Liu, W. Dong, L. Merbold, B. Law, A. Arain, and J. Beringer. 2014. "Global Comparison of Light Use Efficiency Models for Simulating Terrestrial Vegetation Gross Primary Production Based on the LaThuile Database." *Agricultural and Forest Meteorology* 192: 108–120. doi:10.1016/j.agrformet.2014.03.007.

Zhang, L., D. Zhou, J. Fan, and Z. Hu. 2015. "Comparison of Four Light Use Efficiency Models for Estimating Terrestrial Gross Primary Production." *Ecological Modelling* 300: 30–39. doi:10.1016/j.ecolmodel.2015.01.001.

Zhao, M., and S. W. Running. 2010. "Drought-Induced Reduction in Global Terrestrial Net Primary Production from 2000 through 2009." *Science* 329 (5994): 940–943. doi:10.1126/science.1192666.

Zhou, B., Z. Li, X. Wang, Y. Cao, Y. An, Z. Deng, G. Letu, G. Wang, and L. Gu. 2011. "Impact of the 2008 Ice Storm on Moso Bamboo Plantations in Southeast China." *Journal of Geophysical Research: Biogeosciences* 116 (G3). doi:10.1029/2009JG001234.